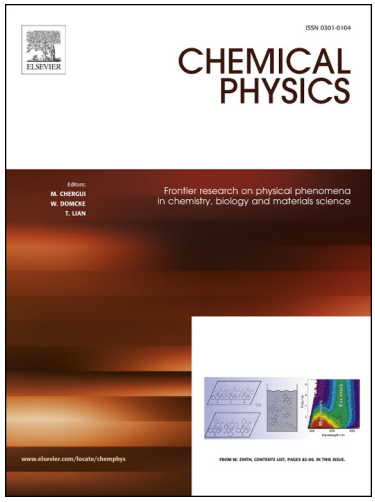

Electronic properties of WS_2 and WSe_2 monolayers with biaxial strain: A first-principles study

Do Muoi, Nguyen N. Hieu, Huong T. T. Phung, Huynh V. Phuc, B. Amin, Bui D. Hoi, Nguyen V. Hieu, Le C. Nhan, Chuong V. Nguyen, P.T.T. Le

PII: S0301-0104(18)31290-4
DOI: https://doi.org/10.1016/j.chemphys.2018.12.004
Reference: CHEMPH 10257

To appear in: *Chemical Physics*

Please cite this article as: D. Muoi, N.N. Hieu, H.T. T. Phung, H.V. Phuc, B. Amin, B.D. Hoi, N.V. Hieu, L.C. Nhan, C.V. Nguyen, P.T.T. Le, Electronic properties of WS_2 and WSe_2 monolayers with biaxial strain: A first-principles study, *Chemical Physics* (2018), doi: https://doi.org/10.1016/j.chemphys.2018.12.004

Electronic properties of WS_2 and WSe_2 monolayers with biaxial strain: A first-principles study

Do Muoi [a,b], Nguyen N. Hieu [c], Huong T. T. Phung [d], Huynh V. Phuc [e], B. Amin [f], Bui D. Hoi [g], Nguyen V. Hieu [h], Le C. Nhan [i], Chuong V. Nguyen [j], P. T. T. Le [k,ℓ,*]

[a] *Department of Physics and Engineering Physics, University of Science-VNU.HCM, Ho Chi Minh City, Viet Nam*

[b] *Department of Natural Sciences, Pham Van Dong University, Quang Ngai, Viet Nam*

[c] *Institute of Research and Development, Duy Tan University, Da Nang, Viet Nam*

[d] *NTT Hi-Tech Institute, Nguyen Tat Thanh University, Ho Chi Minh City, Viet Nam*

[e] *Division of Theoretical Physics, Dong Thap University, Dong Thap, Viet Nam*

[f] *Department of Physics, Hazara University, Mansehra 21300, Pakistan*

[g] *Department of Physics, University of Education, Hue University, Hue, Viet Nam*

[h] *Department of Physics, University of Education, The University of Da Nang, Da Nang, Viet Nam*

[i] *Department of Environmental Sciences, Saigon University, Ho Chi Minh City, Viet Nam*

[j] *Department of Materials Science and Engineering, Le Quy Don Technical University, Ha Noi, Viet Nam*

[k] *Laboratory of Magnetism and Magnetic Materials, Advanced Institute of Materials Science, Ton Duc Thang University, Ho Chi Minh City, Viet Nam*

[ℓ] *Faculty of Applied Sciences, Ton Duc Thang University, Ho Chi Minh City, Viet Nam*

Preprint submitted to Elsevier *11 December 2018*

Abstract

In the present work, we consider electronic properties of WX_2 (X = S, Se) monolayers under a biaxial strain ε_b using the first principles study. Our calculations indicate that, at equilibrium, the WS_2 and WSe_2 monolayers are semiconductors with a direct band gap of respectively 1.800 eV and 1.566 eV while their bulk structures are indirect semiconductors. The electronic properties of the WX_2 monolayers are very sensitive with the biaxial strain, especially compression strain. The biaxial strain ε_b is the cause of the band gap of the WX_2 monolayers and especially the semiconductor–metal phase transition has occurred in the WS_2 monolayer at $\varepsilon_b = -10\%$. In addition, the direct–indirect band gap transition was observed in both WS_2 and WSe_2 monolayers at a certain elongation of biaxial strain ε_b. The phase transitions in these monolayers can be very useful for their applications in nanoelectromechanical devices.

Key words: WS_2, WSe_2, electronic properties, biaxial strain, density functional theory

1 Introduction

Success in the synthesis of two-dimensional (2D) graphene [1] has created a new tendency in the study of layered materials over the past decade. Graphene has attracted an enormous amount of scientists because of its many extraordinary properties [2]. However, due to the zero band gap, graphene has certain limitations in applications in electronic devices [3]. A variety of graphene-like materials have been sought and studied [4–10]. Despite its graphene-like hexagonal structure, transition metal dichalcogenide (TMD) monolayers are a semiconductor material with quite large natural band gap [11, 12]. With natural band gap, TMDs have overcome

* Corresponding author.
Email address: lethithuphuong@tdtu.edu.vn (P. T. T. Le).

the limitations of gapless graphene to become a prospective material for applications in nanoelectronics such as field-effect transistors [13, 14] or detectors [15]. The large spin-orbit-coupling (SOC) energies in the monolayer TMDs due to the contribution of d orbitals of transition metal atoms [16–18] can lead to split degenerate bands.

Among TMD monolayers, the group-VIB TMDs (MoS_2, $MoSe_2$, WS_2, and WSe_2) emerged as the material with many outstanding physical properties such as high mobility at room temperature [19, 20] or controlling their electronic properties easily by an external field and strain engineering [12, 21–24]. Especially, WS_2 and WSe_2 are expected to have many applications in renewable energy technology and energy conversion, particularly the WS_2 monolayer with large band gap around 1.9 eV [25, 26] could be used in the production technology of hydrogen from water [27]. Electronic properties of the monolayers WS_2 and WSe_2 has been investigated by density functional theory (DFT) [4,28,29]. Using the combination of DFT and tight-binding calculations, Roldán and co-workers have considered the effect of the spin-orbit coupling (SOC) on the electronic properties of the monolayers MoS_2 and WS_2 [30]. Similar to graphene, TMD materials are sensitive to external conditions, for instance, strain engineering [12, 31, 32], pressure [33] or defect [34]. While bulks WS_2 and WSe_2 are semiconductors with an indirect band gap, the monolayers WS_2 and WSe_2 are both direct gap semiconductors [25, 28, 35]. The energy gaps of these materials depend strongly on the thickness (number of layers) of the compound [12]. Besides, the strain engineering can strongly modulate the band gap of the monolayers WS_2 and WSe_2 and can even lead to semiconductor–metal phase transition [31]. Effect of strain on electronic properties and phase transition in monolayer WS_2 has been also studied experimentally [36, 37]. In addition to monolayers or multilayers, many scientists have recently focused on heterostructures based on TMDs and other hexagonal materials [38–43] which are many inter-

esting properties that are not found in monolayers [44–47].

In this work, we investigate the influence of the biaxial strain on electronic properties of the WX_2 (X = S, Se) monolayers using the DFT calculations. The electronic states near the Fermi level and the band gap of the monolayers under the biaxial strain are thoroughly also studied and discussed.

2 Model and computational details

In this work, first-principles calculations are employed on basic of the density functional theory to perform the geometric optimization and calculate the electronic properties of bulk and monolayers WX_2 (X = S, Se). All these calculations are realized through Quantum ESPRESSO simulation package [48] within the projector augmented-wave (PAW) pseudopotentials [49,50]. Also, the generalized gradient approximation (GGA) with the Perdew-Burke-Ernzerhof (PBE) parametrization [51,52] was used to delineate the exchange–correlation energy. To describe the van der Waals interactions, which may exist between layers, the DFT-D2 proposed by Grimme (PBE+D2) [53] was used in this study. The first Brillouin zone is sampled with $(15 \times 15 \times 1)$ k-mesh Monkhorst-Pack grid. A kinetic energy cut-off of 500 eV was used in our numerical calculations for plane-wave basis. The structures of the WX_2 (X = S, Se) are fully relaxed with convergence criteria for the force acting on each atom and the total energy respectively being 0.01 eV/Å and 10^{-6} eV. In calculations for the WX_2 monolayers, the vacuum space of 20 Å was used in order to avoid any interaction between the neighbor layers. In the presence of the biaxial strain, we defined the elongation ε_b applying to the monolayer as $\varepsilon_b = (\delta - \delta_0)/\delta_0$, where δ_0 and δ are the unstrained and strained lattice constants, respectively. In this work, the applied biaxial strain ε_b is in the range from -10% to 10%. The minus sign is for the case of compression strain.

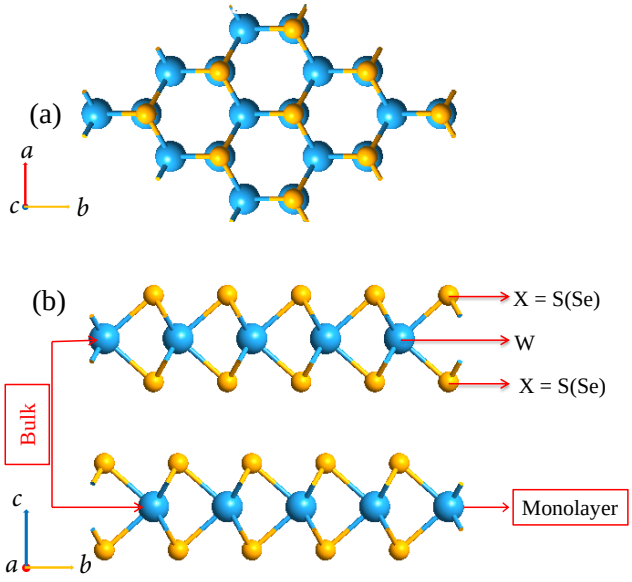

Fig. 1. (a) Top view and (b) side view of the atomic configuration of WX_2 (X = S, Se).

3 Results and discussion

Atomic structure of the WX_2 (X = S, Se) monolayers at equilibrium is shown in Fig. 1. At the equilibrium state, the WX_2 monolayer belongs to the symmetry group D_{3h} with W and X atoms arranged in a hexagonal lattice. In bulk form, the WX_2 monolayers are bonded together by the van der Waals force. Our calculated lattice parameters of both bulk and monolayer WX_2 are listed in Tab. 1. Our results are in good agreement with previous theoretical calculations [28, 54] and experimental measurements [55]. The experimental lattice parameters of the bulk WS_2 are $a_{WS_2} = 3.153$ Å and $c_{WS_2} = 12.323$ Å, and they are $a_{WSe_2} = 3.282$ Å and $c_{WSe_2} = 12.960$ Å in the case of the bulk WSe_2 [55]. Our calculated results for lattice parameters a of the monolayers WS_2 and WSe_2 are respectively 3.185 Å and 3.324 Å which are larger both computational (in this work) and experimental value [55] of the bulk materials.

To investigate the electronic properties, we first calculate the band structure of the bulk WS_2 and WSe_2 at equilibrium as shown in Fig. 2. Our calculations show

Table 1

Structural parameters, total energy, and the band gap of bulk and monolayer WX_2 (X = S, Se) at the equilibrium state

	a, Å	c, Å	Total energy, eV	Band gap, eV
Bulk WS_2	3.167	12.284	−400.911	0.909
Monolayer WS_2	3.185	-	−200.342	1.800
Bulk WSe_2	3.296	12.987	−393.954	0.826
Monolayer WSe_2	3.324	-	−196.952	1.566

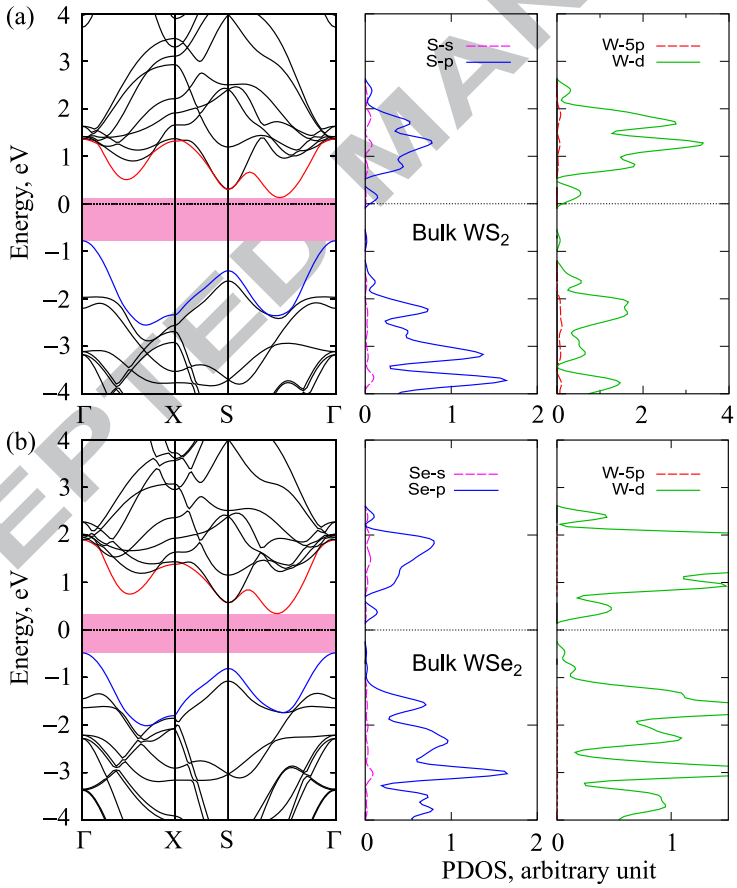

Fig. 2. Band strucure and partial density of states of the bulk WS_2 (a) and WSe_2 (b).

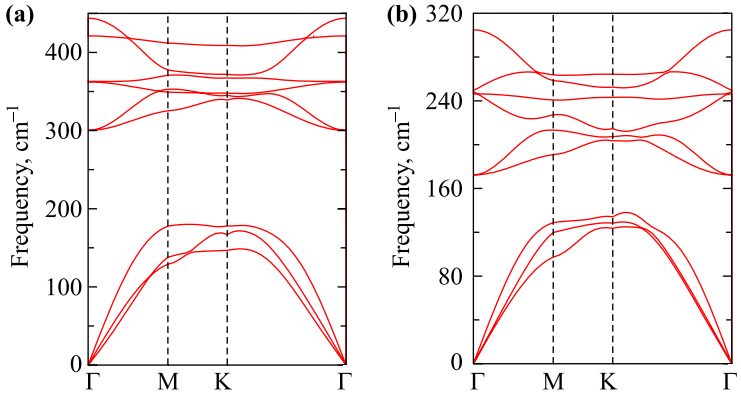

Fig. 3. Phonon dispersion relations of the monolayers WS_2 (a) and WSe_2 (b) at the equilibrium state.

that, in the bulk form, both WS_2 and WSe_2 are semiconductors with an indirect band gap. The indirect energy gap formed between the valence band maximum (VBM) at the Γ-point and the conduction band minimum (CBM) locating on the SΓ-path. As a comparison, we find that the energy gap of the bulk WS_2 (0.909 eV) is slightly larger than that of the bulk WSe_2 (0.826 eV). Our calculated results are in good agreement with the previous DFT calculations [28]. Also, previous experimental measurement has confirmed that the bulk WSe_2 is a semiconductor with an indirect band gap of 1.2 eV [35]. From the partial density of states (PDOS) in the right panel of Fig. 2, we can clearly see the contribution from orbitals of W and X atoms to the energy structure of WX_2. In the bulk WS_2, contribution form the W-d and S-p orbitals to the conduction and valence bands are dominant compared to other orbitals. In a more quantitative view, the W-d contribution to the conduction band was greater than its contribution to the valence band, while the S-p contribution to the valence band was more dominant than its contribution to the conduction band. On the other hand, the contributions of S-s, W-$5p$, and other orbitals is negligible. Similar to the bulk WS_2 case, the energy structure of the bulk WSe_2 is the main contribution from the W-d and Se-p orbitals.

The main task of this work is to focus on the electronic properties monolay-

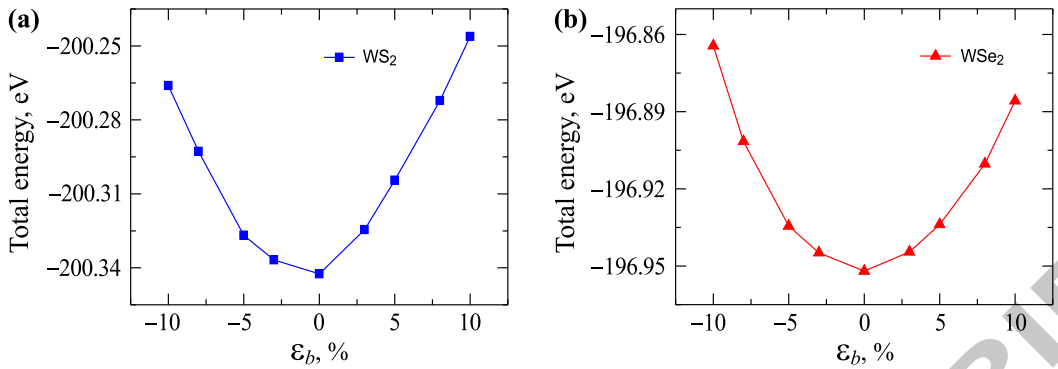

Fig. 4. Dependence of total energy of the monolayers WS_2 (a) and WSe_2 (b) on the biaxial strain ε_b.

ers WX_2 (X = S and Se) in presence of biaxial strain. To begin, we first check the thermodynamic stability of the monolayers. The phonon dispersion relations of the monolayers WS_2 and WSe_2 were calculated and shown in Fig. 3. From Fig. 3, we can see that, in the phonon spectrum of the monolayers, there are no soft phonon modes. This implies that the monolayers WS_2 and WSe_2 at the equilibrium state is stable. At the equilibrium state, the total energy of the WS_2 and WSe_2 monolayers is respectively -200.342 eV and -196.952 eV. Our calculated results demonstrate that the effect of biaxial strain ε_b on the total energy of the monolayers is quite weak. Dependence of the total energy of the monolayers on the ε_b is shown in Fig. 4. In contrast to the bulk structure, our DFT calculations indicate that the monolayers WX_2 are direct semiconductors at the equilibrium state with a larger band gap opening at the S-point. At equilibrium, the band gaps of WS_2 and WSe_2 are respectively 1.800 eV and 1.566 eV. These calculated results agree with the previous theoretical studies [12, 26, 31, 56]. However, the calculated result of the band gap depends strongly on the selected functionals [54]. Electronic energy band structure and PDOS of the WX_2 monolayer at equilibrium are shown in Fig. 5. Similar to the bulk case, the conduction and valence bands near the Fermi level are mainly contribution from the W-d and S-p orbitals. Compared to the bulk case, the

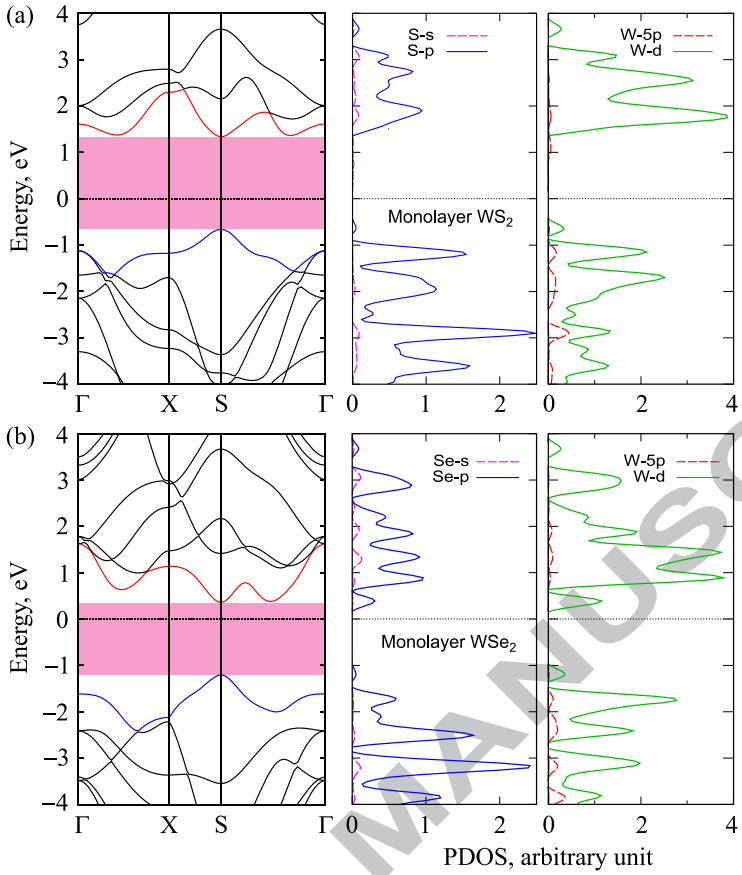

Fig. 5. Band strucure and partial density of states of the monolayers WS_2 (a) and WSe_2 (b).

contribution from S-s, W-5p to the bands of the WS_2 and WSe_2 monolayers was larger but still less significant than the contribution W-d and S-p orbitals. Based on the contribution of the orbital as above-analyzed, therefore, we can bypass these orbitals (such as S/Se-s, W-2p, W-5p) as an approximation to reduce calculations in analytical models, such as tight-binding method, and this neglect does not significantly affect the accuracy of the calculated results, especially when we examine the electronic bands near the Fermi level.

Compared to the bulk case in Fig. 2(b), the conduction band of the WSe_2 monolayer has been significantly changed leading to a difference in the type of band gap (namely, indirect or direct band gap) in these materials. However, focusing on the lowest subband of the conduction band of the monolayer WSe_2, interestingly, we can see that the difference in energy between the CBM and the lowest

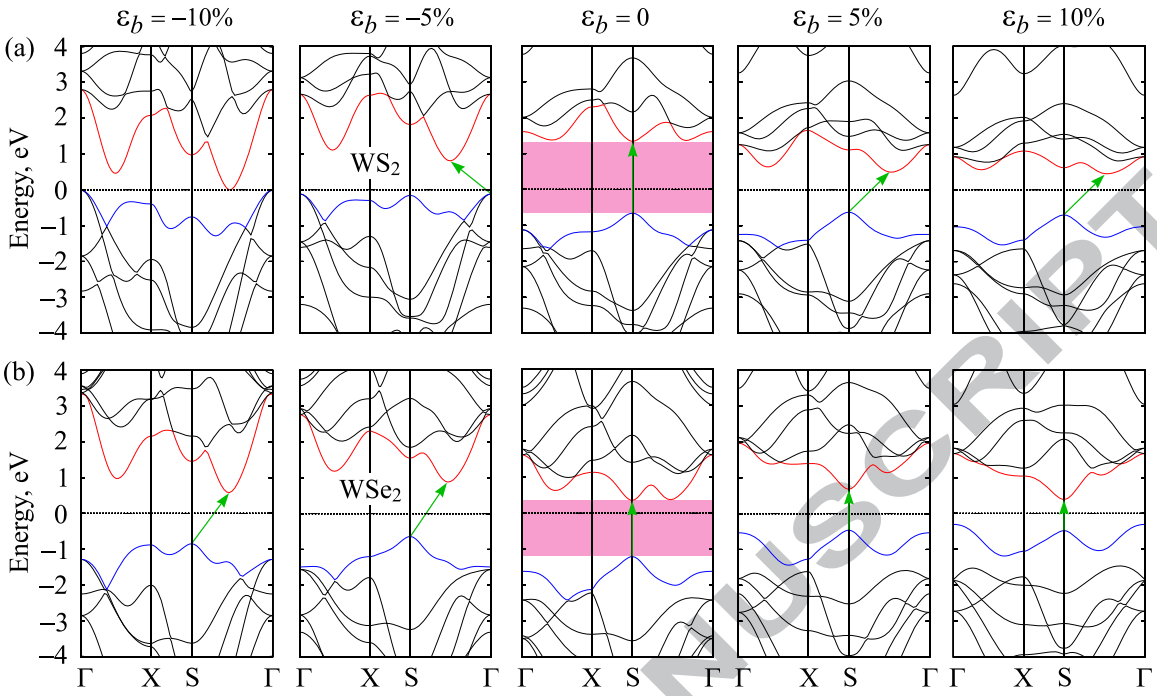

Fig. 6. Band strucure of the monolayers WS_2 (a) and WSe_2 (b) under biaxial strain ε_b.

point of subband part location in the SΓ-path is very small and these two points look like degenerate points. From this, we expect external conditions such as strain engineering or electric field can change these points leading to the direct–indirect band gap transition in the WSe_2 monolayer. In fact, our DFT calculations demonstrate that the band structure of the WX_2 monolayers is very sensitive to the biaxial strain, especially compression case. The band structure of the WX_2 monolayers under biaxial strain ε_b is shown in Fig. 6. From Fig. 6(a), we can interestingly see that the effect of the ε_b on the energy band structure of the monolayer WS_2 is very large. The tensile strain ($\varepsilon_b > 0$) has changed the position of the CBM/VBM leading to the direct–indirect transition as predicted. The monolayer WS_2 becomes an indirect semiconductor under the biaxial strain. In particular, our DFT calculations indicated that the band gap of the monolayer WS_2 decreases rapidly with the presence of the compression biaxial strain and it decreases to zero at $\varepsilon_b = -10\%$. Pressure at biaxial strain of -10% for WSe_2 is 29.43 GPa (and 24.74 GPa for WS_2).

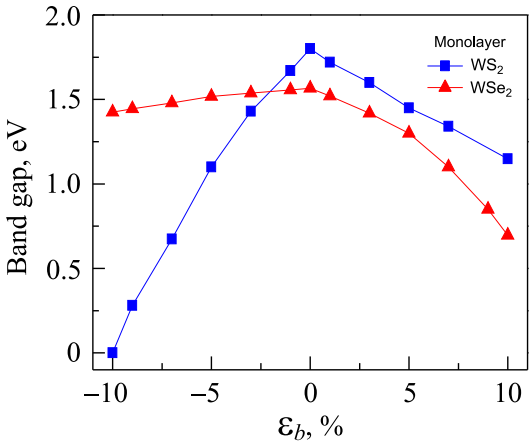

Fig. 7. Dependence of the band gap of the monolayers WS_2 (a) and WSe_2 (b) on the biaxial strain ε_b.

Thus, in addition to the direct–indirect transition, the biaxial strain has resulted in the semiconductor–metal phase transition in the monolayer WS_2 at certain elongation. In the case of the monolayer WSe_2, from Fig. 6(b) we can see that while the tensile biaxial strain does not change the nature of the band gap, the WSe_2 monolayer becomes an indirect semiconductor when the compression biaxial strain is introduced. However, the change in position of the CBM in the monolayer WSe_2 due to the compression biaxial strain leads to the direct–indirect transition, the effect of the compression biaxial strain on the band gap is quite small. Dependence of the band gap of the monolayers WS_2 and WSe_2 on the biaxial strain ε_b is shown in Fig. 7. Clearly, the band gap of both monolayer WSe_2 and WS_2 is reduced in the presence of the ε_b. It means that the band gap of the monolayers WS_2 and WSe_2 is maximum at the equilibrium. The band gap of monolayer WS_2 decreases linearly when the tensile/compression ε_b is applied. In particular, the band gap of the monolayer WSe_2 decreases rapidly when the compression strain is applied and it leads to semiconductor–metal phase transition as mentioned above.

4 Conclusion

In conclusion, we considered the electronic properties of the WX_2 (X = S, Se) monolayers under the biaxial strain ε_b using the DFT calculations. Our calculations have shown that the band gap of the WX_2 monolayers is nearly 2 times the band gap of the bulk WX_2. The electronic properties of the WX_2 monolayers are very sensitive to strain, in particular, we can easily control the band gap of the WX_2 monolayers through the biaxial strain. The biaxial strain does not only lead to direct–indirect band gap in the WX_2 monolayers but also to semiconductor–metal phase transition in the monolayer WS_2. With a wide natural band gap at equilibrium and phase transitions in the presence of strain, the monolayers WX_2 can become a promising material for applications in nanoelectromechanical systems or optoelectronic and photovoltaic devices.

5 Acknowledgments

This research is funded by the Vietnam National Foundation for Science and Technology Development (NAFOSTED) under Grant Number 103.01-2017.309.

References

[1] K. S. Novoselov, A. K. Geim, S. V. Morozov, D. Jiang, Y. Zhang, S. V. Dubonos, I. V. Grigorieva, A. A. Firsov, Science 306 (2004) 666.

[2] E. P. Randviir, D. A. Brownson, C. E. Banks, Mater. Today 17 (2014) 426.

[3] F. Schwierz, Nat. Nanotechnol. 5 (2010) 487.

[4] L. Yi-Hsien, Z. Xin-Quan, Z. Wenjing, C. Mu-Tung, L. Cheng-Te, C. Kai-Di, Y. Ya-Chu, W. J. Tse-Wei, C. Chia-Seng, L. Lain-Jong, L. Tsung-Wu, Adv. Mater. 24 (2012) 2320.

[5] W. Choi, N. Choudhary, G. H. Han, J. Park, D. Akinwande, Y. H. Lee, Mater. Today 20 (2017) 116.

[6] H. D. Bui, M. Yarmohammadi, Phys. Lett. A 382 (2018) 1885.

[7] P. T. T. Le, K. Mirabbaszadeh, M. Davoudiniya, M. Yarmohammadi, Phys. Chem. Chem. Phys. 20 (2018) 25044.

[8] H. D. Bui, M. Yarmohammadi, J. Magn. Magn. Mater. 465 (2018) 646.

[9] H. D. Bui, L. T. T. Phuong, M. Yarmohammadi, Europhys Lett. 124 (2) (2018) 27001.

[10] P.T.T. Le, M. Davoudiniya, K. Mirabbaszadeh, B. D. Hoi, M. Yarmohammadi, Physica E 106 (2019) 250.

[11] G. G. Naumis, S. Barraza-Lopez, M. Oliva-Leyva, H. Terrones, Rep. Prog. Phys. 80 (2017) 096501.

[12] W. S. Yun, S. W. Han, S. C. Hong, I. G. Kim, J. D. Lee, Phys. Rev. B 85 (2012) 033305.

[13] R. Dhall, Z. Li, E. Kosmowska, S. B. Cronin, J. Appl. Phys. 120 (19) (2016) 195702.

[14] A. Nourbakhsh, A. Zubair, R. N. Sajjad, A. Tavakkoli K. G., W. Chen, S. Fang, X. Ling, J. Kong, M. S. Dresselhaus, E. Kaxiras, K. K. Berggren, D. Antoniadis, T. Palacios, Nano Lett. 16 (2016) 7798.

[15] O. Lopez-Sanchez, D. Lembke, M. Kayci, A. Radenovic, A. Kis, Nat. Nanotechnol. 8 (2013) 497.

[16] X. Xu, W. Yao, D. Xiao, T. F. Heinz, Nat. Phys. 10 (2014) 343.

[17] M. Yarmohammadi, J. Electron. Mater. 45 (2016) 4958.

[18] B. D. Hoi, M. Yarmohammadi, J. Magn. Magn. Mater. 451 (2018) 57.

[19] H. Fang, S. Chuang, T. C. Chang, K. Takei, T. Takahashi, A. Javey, Nano Lett. 12 (2012) 3788.

[20] W. Bao, X. Cai, D. Kim, K. Sridhara, M. S. Fuhrer, Appl. Phys. Lett. 102 (2013) 042104

[21] C. V. Nguyen, N. N. Hieu, Chem. Phys. 468 (2016) 9.

[22] K. V. Shanavas, S. Satpathy, Phys. Rev. B 91 (2015) 235145.

[23] M. Yarmohammadi, J. Magn. Magn. Mater. 426 (2017) 621.

[24] B. D. Hoi, M. Yarmohammadi, K. Mirabbaszadeh, Superlattices Microstruct. 104 (2017) 331.

[25] A. Kuc, N. Zibouche, T. Heine, Phys. Rev. B 83 (2011) 245213.

[26] Y. Ma, Y. Dai, M. Guo, C. Niu, J. Lu, B. Huang, Phys. Chem. Chem. Phys. 13 (2011) 15546.

[27] J. Nowotny, C. Sorrell, L. Sheppard, T. Bak, Int. J. Hydrog. Energy 30 (2005) 521.

[28] R. Roldán, J. A. Silva-Guillén, M. P. López-Sancho, F. Guinea, E. Cappelluti, P. Ordejón, Annalen de Physics 526 (2014) 347

[29] D. A. Ruiz-Tijerina, M. Danovich, C. Yelgel, V. Zólyomi, V. I. Fal'ko, Phys. Rev. B 98 (2018) 035411.

[30] R. Roldán, M. P. López-Sancho, F. Guinea, E. Cappelluti, J. A. Silva-Guillén, P. Ordejón, 2D Mater. 1 (2014) 034003.

[31] A. E. Maniadaki, G. Kopidakis, I. N. Remediakis, Solid State Commun. 227 (2016) 33.

[32] Á. M. García, E. d. Corro, M. Kalbac, O. Frank, Phys. Chem. Chem. Phys. 19 (2017) 13333.

[33] X. Su, R. Zhang, C. Guo, J. Zheng, Z. Ren, Phys. Lett. A 378 (2014) 745.

[34] Z. Lin, B. R. Carvalho, E. Kahn, R. Lv, R. Rao, H. Terrones, M. A. Pimenta, M. Terrones, 2D Mater. 3 (2016) 022002.

[35] M. Traving, M. Boehme, L. Kipp, M. Skibowski, F. Starrost, E. E. Krasovskii, A. Perlov, W. Schattke, Phys. Rev. B 55 (1997) 10392.

[36] Y. Wang, C. Cong, W. Yang, J. Shang, N. Peimyoo, Y. Chen, J. Kang, J. Wang, W. Huang, T. Yu, Nano Res. 8 (2015) 2562.

[37] J. Krustok, R. Kaupmees, R. Jaaniso, V. Kiisk, I. Sildos, B. Li, Y. Gong, AIP Adv. 7 (2017) 065005.

[38] H. V. Phuc, N. N. Hieu, B. D. Hoi, L. T. Phuong, C. V. Nguyen, Surf. Sci. 668 (2018) 23.

[39] K. D. Pham, H. V. Phuc, N. N. Hieu, B. D. Hoi, C. V. Nguyen, AIP Adv. 8 (2018) 075207.

[40] M. Sun, J.-P. Chou, J. Yu, W. Tang, Phys. Chem. Chem. Phys. 19 (2017) 17324.

[41] S. Wang, C. Ren, H. Tian, J. Yu, M. Sun, Phys. Chem. Chem. Phys. 20 (19) (2018) 13394.

[42] S. Li, M. Sun, J.-P. Chou, J. Wei, H. Xing, A. Hu, Phys. Chem. Chem. Phys. 20 (2018) 24726.

[43] S. Wang, H. Tian, C. Ren, J. Yu, M. Sun, Sci. Rep. 8 (2018) 12009.

[44] M. Sun, J.-P. Chou, Y. Zhao, J. Yu, W. Tang, Phys. Chem. Chem. Phys. 19 (2017) 28127.

[45] Z. Cui, X. Wang, E. Li, Y. Ding, C. Sun, M. Sun, Nanoscale Res. Lett. 13 (2018) 207.

[46] Y. Luo, C. Ren, S. Wang, S. Li, P. Zhang, J. Yu, M. Sun, Z. Sun, W. Tang, Nanoscale Res. Lett. 13 (2018) 282.

[47] M. Sun, J.-P. Chou, J. Gao, Y. Cheng, A. Hu, W. Tang, G. Zhang, ACS Omega 3 (2018) 8514.

[48] P. Giannozzi, S. Baroni, N. Bonini, M. Calandra, R. Car, C. Cavazzoni, D. Ceresoli, G. L. Chiarotti, M. Cococcioni, I. Dabo, A. D. Corso, S. de Gironcoli, S. Fabris, G. Fratesi, R. Gebauer, U. Gerstmann, C. Gougoussis, A. Kokalj, M. Lazzeri, L. Martin-Samos, N. Marzari, F. Mauri, R. Mazzarello, S. Paolini, A. Pasquarello, L. Paulatto, C. Sbraccia, S. Scandolo, G. Sclauzero, A. P. Seitsonen, A. Smogunov, P. Umari, R. M. Wentzcovitch, J. Phys.: Condens. Matter 21 (2009) 395502.

[49] P. E. Blöchl, Phys. Rev. B 50 (1994) 17953.

[50] G. Kresse, D. Joubert, Phys. Rev. B 59 (1999) 1758.

[51] J. P. Perdew, K. Burke, M. Ernzerhof, Phys. Rev. Lett. 77 (1996) 3865.

[52] J. P. Perdew, K. Burke, M. Ernzerhof, Phys. Rev. Lett. 78 (1997) 1396.

[53] S. Grimme, J. Computat. Chem. 27 (15) (2006) 1787.

[54] Y. Ding, Y. Wang, J. Ni, L. Shi, S. Shi, W. Tang, Physica B 406 (2011) 2254.

[55] W. Schutte, J. De Boer, F. Jellinek, J. Solid State Chem. 70 (1987) 207.

[56] W. Huang, X. Luo, C. K. Gan, S. Y. Quek, G. Liang, Phys. Chem. Chem. Phys. 16 (22) (2014) 10866.